ELSEVIER

Kinetics of Human Acetylcholinesterase Inhibition by the Novel Experimental Alzheimer Therapeutic Agent, Tolserine

Mohammad A. Kamal,* Nigel H. Greig,† Abdullah S. Alhomida* and Abdulaziz A. Al-Jafari‡

*DEPARTMENT OF BIOCHEMISTRY, COLLEGE OF SCIENCE, KING SAUD UNIVERSITY, RIYADH, SAUDI ARABIA; AND †DRUG DESIGN & DEVELOPMENT, NATIONAL INSTITUTE OF AGING, NATIONAL INSTITUTE OF HEALTH, BALTIMORE, MARYLAND 21224, U.S.A.

ABSTRACT. Characterization of the kinetic parameters of tolserine, a novel acetylcholinesterase (AChE) inhibitor of potential in the therapy of Alzheimer's disease, to inhibit purified human erythrocyte AChE was undertaken for the first time. An IC_{50} value was estimated by three methods. Its mean value was found to be 8.13 nM, whereas the IC_{100} was observed to be 25.5 nM as calculated by single graphical method. The Michaelis–Menten constant (K_m) for the hydrolysis of the substrate acetylthiocholine iodide was found to be 0.08 mM. Dixon as well as Lineweaver–Burk plots and their secondary replots indicated that the nature of the inhibition was of the partial non-competitive type. The value of K_i was estimated as 4.69 nM by the primary and secondary replots of the Dixon as well as secondary replots of the Lineweaver–Burk plot. Four new kinetic constants were also investigated by polynomial regression analysis of the relationship between the apparent K_i (K_{Iapp}) and substrate concentration, which may open new avenues for the kinetic study of the inhibition of several enzymes by a wide variety of inhibitors *in vitro*. Tolserine proved to be a highly potent inhibitor of human AChE compared to its structural analogues physostigmine and phenserine. BIOCHEM PHARMACOL **60**;4:561–570, 2000. © 2000 Elsevier Science Inc.

KEY WORDS. acetylcholinesterase; Alzheimer's disease; inhibition; kinetics; novel; tolserine

Whereas several neurotransmitter systems are involved and depleted in Alzheimer's disease (AD§), the cholinergic system still receives by far the greatest attention, particularly with regards to pharmacotherapeutic research and development [1, 2], due to its involvement in learning and memory processing [3]. Pharmacologic strategies for AD treatment have focused on increasing cholinergic neurotransmission via direct stimulation of muscarinic [4] and nicotinic receptors [5], and via inhibition of AChE (3.1.1.7) [2]. AChE is the principle enzyme involved in the hydrolysis of acetylcholine (ACh) to end its action in neural synapses [6]. Inhibition of AChE increases extracellular levels of ACh and thereby amplifies its action [1]. This counteracts the synaptic loss in the AD brain, the major correlate of cognitive impairment [7]. It is possible that agents that alter the inappropriate proteolytic processing of the APP in individuals with AD, will contribute to halting the disease. However, this is a hypothesis that has yet to be fully tested. Neurogenetic studies and the development of transgenic animals strongly indicate that in familial AD, the misprocessing of APP and the generation of β-amyloid peptide is related to the disease process. At present, however, there is no definitive proof that this is so or that it is the only factor that accounts for the vast majority of sporadic AD individuals.

The development of cholinesterase inhibitors, ChEIs, has thus far proved to be the most rewarding approach for AD treatment, with two drugs presently available for wide clinical use. These are tacrine (Cognex™, Warner-Lambert), a short-acting and non-selective ChEI that is associated with a high incidence of reversible hepatotoxicity [8, 9], and donepezil (Aricept™, Pfizer), a recently approved AChE inhibitor that is better tolerated than tacrine and has proven more effective in alleviating the cognitive deficits associated with AD, particularly in patients with early- to mid-stage disease [10]. Tacrine and donepezil represent two of more than a dozen ChEIs that are presently in clinical and preclinical development for AD [1]. Clearly, not all will make it into the market place as prescription drugs.

Simplistically, ChEIs can be broadly separated into first-,

‡ Corresponding author: Prof. Abdulaziz A. Al-Jafari, Department of Biochemistry, College of Science, King Saud University, P.O. Box 2455, Riyadh, 11451, Saudi Arabia. Tel. 966-1-4675953; FAX 966-1-467-5791; E-mail: jafari@ksu.edu.sa
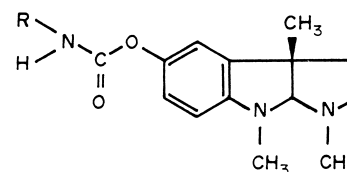
§ *Abbreviations:* AChE, acetylcholinesterase; AD, Alzheimer's disease; APP, amyloid precursor protein; ASCh, acetylthiocholine iodide; BChE, butyrylcholinesterase; ChEIs, cholinesterase inhibitors; DTNB, 5,5′-dithiobis-2-nitrobenzoic acid; IC_{100}, that concentration of the inhibitor that causes 100% inhibition of the enzyme activity; K_{Iapp}, apparent K_i; K_{mapp}, apparent K_m; V_{maxapp}, apparent V_{max} at the given concentration of tolserine; and $V_{maxiapp}$, apparent V_{max} at the given concentration of ASCh.

second-, and third-generation agents based on their pharmacologic profiles, with the third generation possessing specific advantages over the earlier ones. First-generation agents such as tacrine and physostigmine are classical ChEIs that were not designed for AD and are short-acting (duration 2 to 3 hr) and unselective between the two ChEI subtypes, AChE and BChE (3.1.1.8). Second-generation agents possess either a long duration of action, i.e. metrifonate (Bayer) or eptylstigmine (Mediolanum), or a selectivity for AChE inhibition, i.e. donepezil [1, 11]. In contrast, third-generation compounds possess both these attributes and potentially others too, such as an ability to alter other pathological processes involved in AD. It is clear that specific ChEIs alter the processing of APP and reduce the production and secretion of β-amyloid peptide (and as described above, this may impact on the disease process). Recent studies indicate that this is true for the third-generation drugs phenserine and tolserine [12]. This is also true for tacrine, albeit at high concentrations [13, 14]. This action is unrelated to the action of the compounds on cholinesterase, as other ChEIs do not have this action (e.g. physostigmine and metrifonate) [14]. Hence, drug design and development efforts are being focused at this target in the hope that it is a clinically relevant one.

We have recently described the enzyme kinetics of phenserine, a third-generation AChE inhibitor that is entering phase I clinical trials, against human erythrocyte AChE [15]. This novel agent is rapidly cleared from the body (half-life 10 min), but possesses an extended duration of selective AChE inhibitory action (greater than 8 hr). Recent research indicates that selective inhibitors of AChE do not have the aberrant side effect profile of non-selective ChEIs [16] and, in this regard, phenserine possessed an unusually wide therapeutic window in preclinical cognitive studies in rodents [17, 18]. Furthermore, the compound reaches 10-fold higher levels in brain versus plasma and possesses the ability to interact in the molecular events leading to AD by altering the processing of β-APP to reduce generation of the neurotoxic AD peptide, β-amyloid [19], in animal studies [20].

We describe herein the enzyme kinetics of tolserine, a close analogue of phenserine that differs by a single 2′-methyl substitution on its phenylcarbamoyl moiety (Fig. 1). It is this part of the compound that specifically interacts and carbamylates AChE to inhibit its ability to bind and cleave substrates. Tolserine has likewise demonstrated an unusually high potency to augment memory and cognition in preliminary rodent studies [21]. Like phenserine, tolserine is rapidly cleared from the body and possesses a long duration of action (greater than 8 hr). The single substitution in phenserine to provide tolserine, however, provides it with a dramatic selectivity for AChE versus BChE of 200-fold, and a high brain uptake (brain/plasma concentration ratio of 24:1). In light of our prior studies on phenserine, we assess in the present report how this minor 2′-phenylcarbamoyl substitution affects the binding kinetics of tolserine to human AChE.
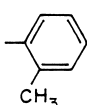

FIG. 1. Chemical structures of physostigmine (eserine) and its two derivatives (phenserine and tolserine).

MATERIALS AND METHODS
Materials

ASCh (used as substrate), human erythrocyte AChE (Type XIII), and DTNB were purchased from Sigma Chemical Co. BSA was obtained from Fluka Chemika-BioChemika. Tolserine, (−)-2′-methyl-phenyl-carbamoyleseroline, was synthesized as reported earlier [22] and was prepared as its water-soluble L-tartrate salt. It was optically and chemically pure (>99.9%).

Assay of AChE Activity

AChE activity was measured at 22° by the Ellman method [23]. The assay mixture contained 0.25 mM ASCh, 0.25 mM DTNB, and 50 mM sodium phosphate buffer. The remaining assay conditions have been reported previously [24]. For the selection of a suitable concentration of AChE, at which the relationship between initial velocity (v) and total enzyme concentration should be linear, 0.20–3.20 μg/mL of AChE was assayed *in vitro* from 2 to 20 min under the same conditions of temperature, pH, and components of the assay mixtures. The rate of change of substrate cleavage, determined by measuring the absorbance of the reaction product at 412-nm wavelength, was measured at different time intervals. The product was calculated for each [AChE] at 4-min incubation time intervals. To study the effect of tolserine on AChE substrate cleavage, the enzyme was preincubated with tolserine for 10 min prior to the addition of substrate.

Computation of IC_{50} and IC_{100}

The first method for the estimation of IC_{50} was applied by transformed data of log of V_{map}/V_m-V_{map} versus log [tol-

serine] (1.25–20.0 nM), where V_{map} equals the maximum apparent velocity of the AChE in the presence of tolserine and V_m is equal to V_{max} (i.e. the maximum velocity in the absence of tolserine). This, according to our knowledge, is a new method to determine the value of IC_{50}; the calculations of (i) $v/V_{max}-v$ (where V_{max} is equal to the maximum velocity in the absence of inhibitor and v is the activity in the presence of inhibitor) versus [substrate], i.e. Hill plot [25], and (ii) log v/v_o-v (where v_o = velocity in the absence of inhibitor and v in the presence of inhibitor) versus log [inhibitor] are already known [26, 27]. The benefit of this new applied method lies in its providing a precise IC_{50} value regardless of any particular substrate concentration due to its reliance on maximum velocity and maximum apparent velocity, which are an index of the activity of the enzyme at overall substrate concentrations (low to high concentrations). In some cases, the IC_{50} value can change with respect to a change in the substrate concentration. In such a case, this value should be determined at each individual concentration; however, this problem can readily be solved by estimating the IC_{50} according to the new procedure adopted in the present study. With this method, the IC_{50} was determined in two ways: (i) calculation by linear regression analysis and (ii) by plotting the intersection line at the x-axis with the naked eye after enlarging the graph.

The third method was also interesting, because it was modified by combining two conventional methods, i.e. the plotting of percent activity or % inhibition of enzyme inhibited by inhibitor versus inhibitor concentration individually. In the current study, however, plots for % activity as well as % inhibition were plotted together in the same graph versus tolserine concentration (1.25–40.0 nM). This simple graph verified the value of IC_{50} that was estimated by the two methods described earlier in the current study. Moreover, one further fruitful parameter was also obtained by this type of analysis; specifically, an IC_{100} value (the concentration that causes 100% inhibition of AChE). This was calculated graphically from the same plot by drawing a vertical line from the point where the AChE activity reached a zero value as well as a 100% inhibition to the x-axis ordinate.

Estimation of Kinetic Parameters, Protein, and Statistical Analysis

Michaelis constants (K_m) were determined by means of Lineweaver–Burk plots using initial velocities obtained over a substrate concentration range of between 0.025 and 0.25 mM. The assay conditions for determining the residual activities in the presence of tolserine were identical to the above assay procedure, except that a fixed concentration (2.50–20.0 nM) of tolserine was used in the assay medium. The protein content of the enzyme preparation was estimated according to the method of Lowry *et al.* [28], using BSA as a standard. Graphs were plotted by using two programs, GraFit [29] and Prism V2.0, GraphPad Software Inc. The values of the correlation coefficient, slope, inter-
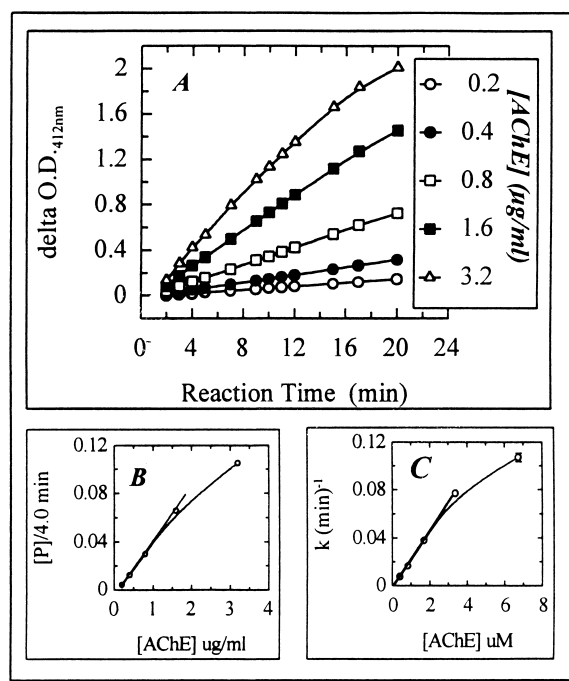

FIG. 2. AChE assays: (A) product formation as a function of time at different concentrations of AChE as indicated in legend box. (B) initial velocity (calculated as product concentration per 4.0 min) as a function of enzyme concentration. (C) Slope (k) of each plot for each concentration of AChE in Fig. 2A versus its enzyme concentration.

cept, and their standard errors were obtained by linear and non-linear regression analysis using these programs.

RESULTS

The data shown in Fig. 2 were used to determine the limits of linearity with regard to product concentration versus incubation time for different amounts of AChE. It can be seen that product concentration was constant for all enzyme concentrations (0.2–3.2 μg/mL) up to time 4.0 min (Fig. 2A). Thereafter, the response was not linear for any except the 0.20 μg/mL and 0.40 μg/mL concentrations. Therefore, the product concentration of each concentration of AChE was determined at 4.0 min and was then plotted against [AChE] (Fig. 2B). The rate of product formation (k) was constant from 0.20–1.60 μg/mL of [AChE] (Fig. 2C). The correlation coefficient was calculated as 1.0 for 0.20–1.60 μg/mL of [AChE] with a slope value of 0.024 ± 0.0003 $(\mu M.min)^{-1}$. As a consequence, a concentration of 0.80 μg/mL of AChE and an incubation time of 4.0 min were chosen as suitable conditions to provide for linearity of AChE activity in further kinetic studies.

The transformed data for the inhibition of human erythrocyte AChE as a function of tolserine concentration are presented in Fig. 3, A and B. The results show by three methods, as discussed in the methodology section, that tolserine inhibits AChE activity in a concentration-depen-
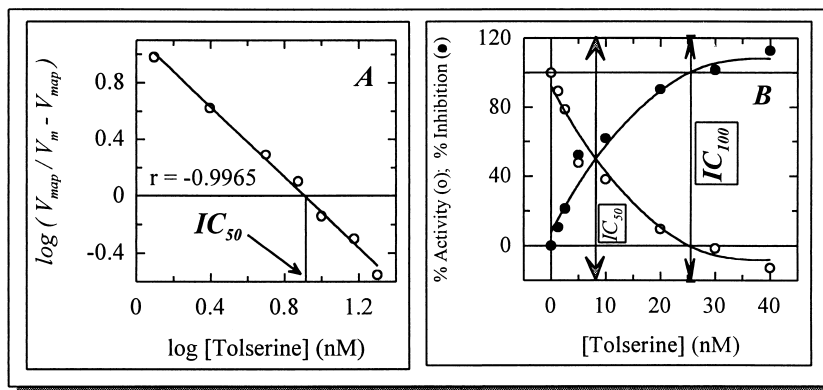
FIG. 3. Human erythrocyte AChE inhibition by tolserine. Transformed data are presented in the resemblance form to a Hill plot, where V_{map} and V_m are the maximal reaction rates for the experimental and control systems, respectively. Each point is the mean of three independent determinations.

dent manner, with IC_{50} values of 8.096, 8.128, and 8.15 nM and a mean value of 8.13 ± 0.016 nM, while the IC_{100} value was 25.5 nM.

The nature of the inhibition of AChE activity by tolserine is shown in Fig. 4. Inhibition was found to be of a non-competitive type (Fig. 4A). Specifically, tolserine decreased V_{max} (19.2–78.1%) without producing a significant change in the value of K_m (Table 1). The K_m value for human erythrocyte AChE was calculated by three methods. The first was from the intersection at the abscissa (Fig. 4A), the second from the intersection of $1/V_{maxipp}$, and the third from the slope plots at the abscissa (Fig. 6A). The mean

value of these was 0.08 ± 0.004 mM. Apparent values of V_{max} were determined by linear regression analysis of $1/v$ versus $1/[ASCh]$ data from the Lineweaver–Burk plot over a substrate concentration range between 0.025 and 0.25 mM and at a tolserine concentration of between 2.5 and 20.0 nM (Fig. 4A). A model for equilibria between different forms of the AChE (free, combined with ASCh or tolserine, or acetylated [Ac]) for this partial non-competitive type of inhibition system is as shown in Scheme 1. A reciprocal form of the kinetic equation for the presentation of velocity in this type of inhibition system is as follows:
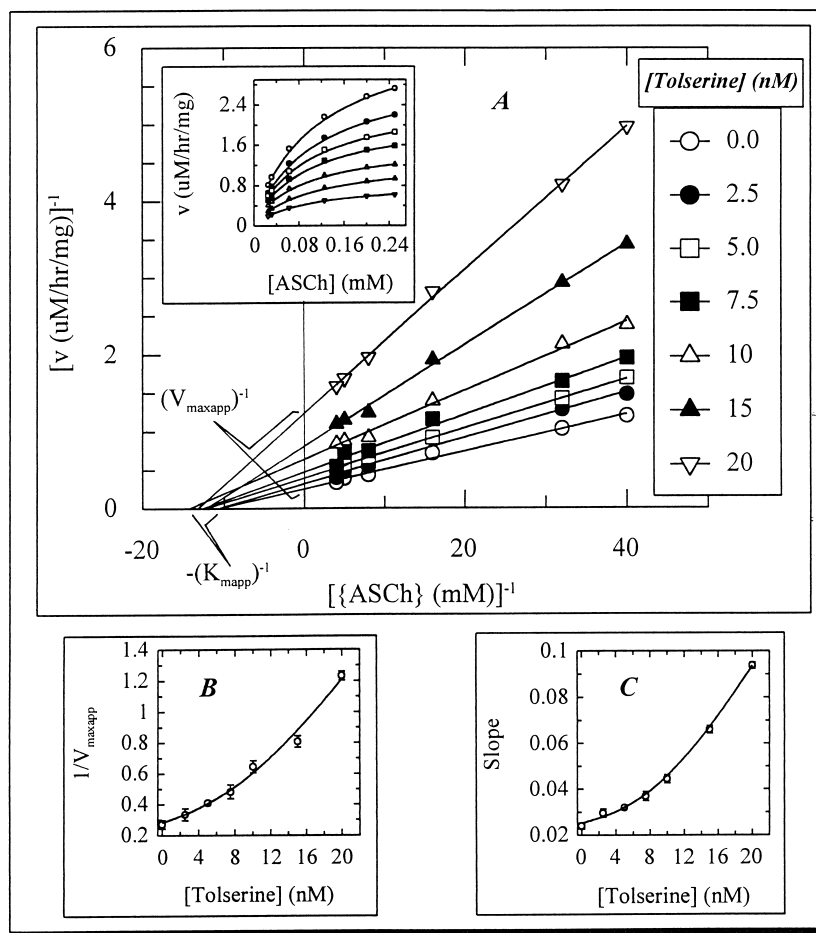

FIG. 4. (A) Lineweaver–Burk plots representing the reciprocal of initial enzyme velocity versus the reciprocal of ASCh concentration in the absence and presence of different concentrations of tolserine (0–20 nM) as shown in legend box. K_{mapp} is an apparent K_m for each concentration of the tolserine. The correlation coefficients were 0.995, 0.993, 1.0, 0.994, 0.997, 0.999, and 1.0 for 0.0, 2.5, 5.0, 7.5, 10.0, 15.0, and 20.0 nM tolserine concentrations, respectively. (Inset) Hyperbolic plots representing initial AChE velocity versus ASCh concentration in the absence and presence of tolserine. (B and C) Secondary replots of Lineweaver–Burk plot: $1/V_{maxapp}$ and slope versus tolserine concentrations. The bar on each point represents the value of SD obtained by linear regression analysis of plots in Fig. 4A.

TABLE 1. Effect of tolserine on K_m and V_{maxapp} of purified human erythrocyte AChE

Tolserine (nM)	K_{mapp} (mM)	V_{maxapp} μM/hr/mg)	Percent decrease
0	0.088	3.70	0
2.5	0.088	2.99	19.16
5.0	0.078	2.45	34.04
7.5	0.077	2.07	43.91
10.0	0.069	1.55	58.01
15.0	0.082	1.24	66.53
20.0	0.076	0.81	78.06

The K_{mapp} and V_{maxapp} were determined by their respective regression equations (Fig. 4A).
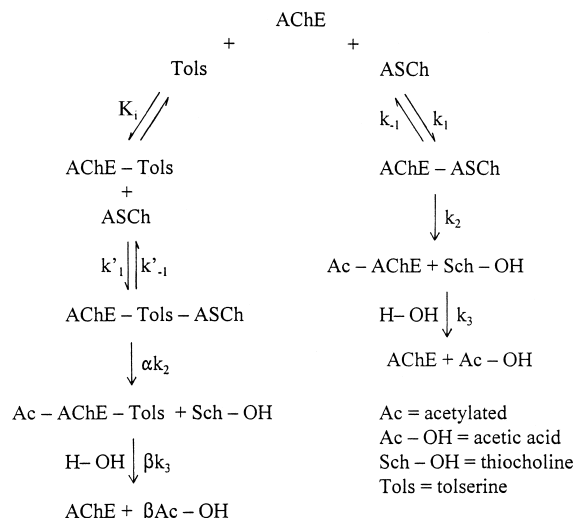
$$1/v = 1/V_{max}[\{1+(Tols)/K_i\}/\{1+\beta(Tols)/K_i\}]$$

$$+ K_m/V_{max}[\{1+(Tols)/K_i\}/\{1 + \beta(Tols)/K_i\}]$$

$$\times 1/[ASCh] \quad (1)$$

$$K_m = k_{-1}+k_2+k_3/k_1 \quad (2)$$

$$K_{mapp} = k'_{-1} + \alpha k_2 + \beta k_3/k'_1 \quad (3)$$

where Tols denotes tolserine.

$V_{maxiapp}$ was determined by three methods, subplot of Fig. 5, A–C; in the case of (B), it is equal to the intersection of each line for each ASCh concentration on the ordinate, while the reciprocal of y-axis intersection of each line in Fig. 5, A and C and the mean value is presented in Table 2. The value of the K_i (the dissociation constant of the AChE–tolserine complex into free AChE and tolserine) was determined directly from the intersection of the line for each substrate concentration on the abscissa of Fig. 5C. Over the range of ASCh concentrations used (0.025–0.25 mM), there was an increase in $V_{maxiapp}$ of between 16.5% and 256.0%, while there was no significant change in the K_{Iapp} value. The inhibition constant, K_i, was calculated by four methods. First, $1/V_{maxapp}$ was calculated at each

concentration of tolserine (Fig. 4A) and then was plotted against tolserine concentration (Fig. 4B). Second, the slope of each Lineweaver–Burk plot (Fig. 4A) was plotted against tolserine concentration (Fig. 4C); the K_i was calculated from the abscissa. Third, the K_{Iapp} was calculated by linear regression analysis from data in the Dixon plot (Fig. 5C) and replotted against $1/[ASCh]$ as presented in Fig. 6B. Finally, as a fourth method, the K_{Iapp} was replotted against the ASCh concentration, as presented in Fig. 6C. It should be noted that Fig. 6, B and C is comprised of a newly introduced relationship between K_{Iapp} and substrate concentrations [15]. These values for the K_i, calculated by the described methods, are shown together with a derived mean value in Table 3. The polynomial regression analysis of the secondary replot of the Dixon plot, i.e. Fig. 6, B and C (curve lines), is noteworthy as it obtains the following new kinetic constants:

$$Ka_{K_{Iapp} vs 1/[S]} = 3.7 \pm 0.3 \text{ nM}$$

SCHEME 1. Equilibria for a partial non-competitive type of inhibition system.

Ac = acetylated
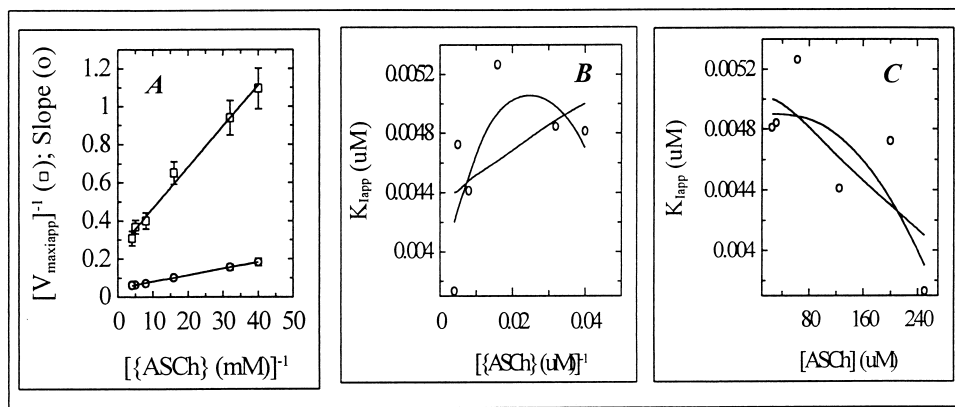Ac – OH = acetic acid
Sch – OH = thiocholine
Tols = tolserine

FIG. 6. Secondary replot of the Dixon plot: (A) $1/V_{maxiapp}$ and slope of the lines in Dixon plot versus reciprocal of the ASCh concentrations, where the correlation coefficients were 0.995 and 0.999, respectively. The bar on each point represents the value of SD obtained by linear regression analysis of plots in Fig. 5C. (B) Represents a relationship of K_{Iapp} with reciprocal of the substrate concentration. (C) A plot of scattered K_{Iapp} values at each substrate concentration against the substrate concentrations. Straight and curved lines show linear regression and polynomial regression analysis, respectively.
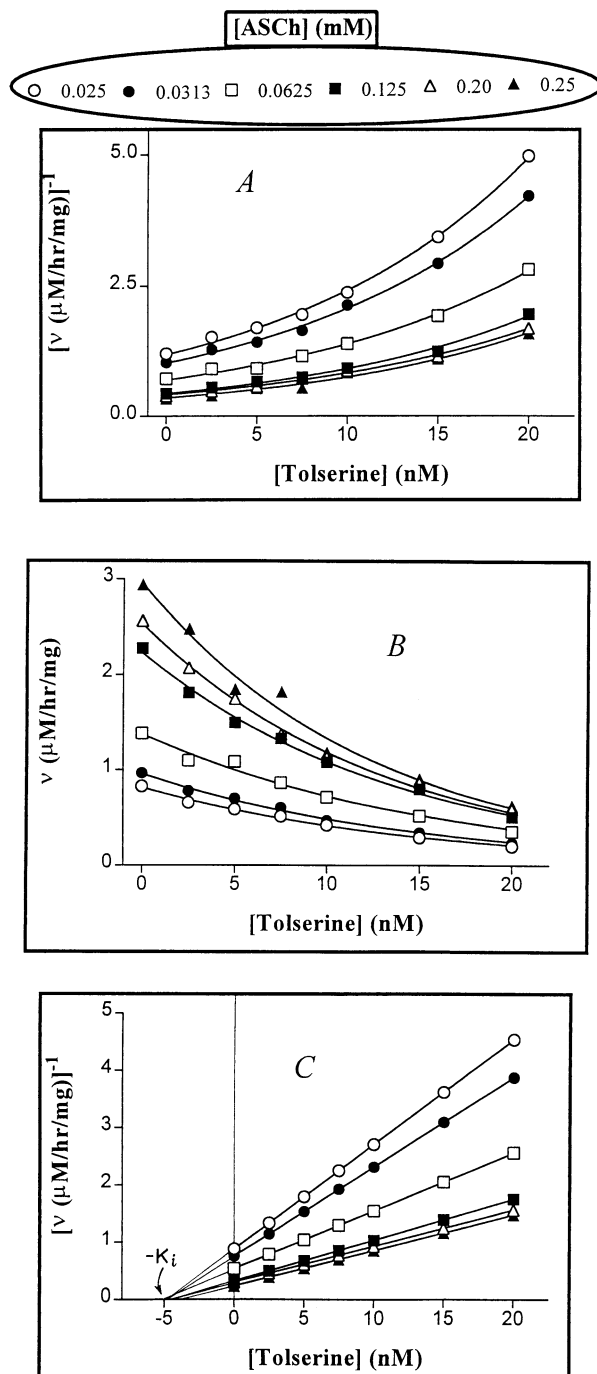
FIG. 5. Dixon plot for human erythrocyte AChE at six ASCh concentrations as indicated in legend box. (A) Presentation of experimental data of the inhibition pattern after non-linear regression analysis. Correlation coefficients $(r)^2$ were 0.998, 0.998, 0.996, 0.994, 0.996, and 0.987 for o, ●, □, ■, △, and ▲, respectively. (B) Representing initial AChE velocity versus different concentrations of tolserine (0–20 nM) at six fixed concentrations of substrate as shown in legend box. This plot usually distinguishes pure non-competitive inhibition from partial inhibition [48]. The r^2 were 0.994, 0.994, 0.981, 0.995, 0.996, and 0.980 for o, ●, □, ■, △, and ▲, respectively according to non-linear regression analysis. (C) Representing the reciprocal of initial velocity of AChE versus different concentrations of tolserine after linear regression analysis. The correlation coefficients were 0.973, 0.976, 0.971, 0.967, 0.983, and 0.978 for o, ●, □, ■, △, and ▲, respectively.

TABLE 2. Effect of tolserine on K_{Iapp} and $V_{maxiapp}$ of purified human erythrocyte AChE

[ASCh] (mM)	K_{Iapp} (nM)	$V_{maxiapp}$ (μM/hr/mg)	% increase
0.025	4.81	0.91	0.0
0.031	4.84	1.06	16.48
0.063	5.26	1.53	68.13
0.125	4.41	2.50	174.73
0.200	4.72	2.71	197.80
0.250	3.73	3.24	256.04

The K_{Iapp} was determined by its respective regression equation in Dixon plot (Fig. 5C). The K_{Iapp} is equal to x-axis intersection, while $V_{maxiapp}$ is the mean of $V_{maxiapp}$ estimated from three subplots (Fig. 5, A–C). It is equal to the y-intersection of each line for each ASCh concentration in the case of B, while it is the reciprocal of y-intersection of each line in the Fig. 5, A and C.

$$Kb_{Klapp \, vs \, 1/[S]} = 125.1 \pm 14.9 \, (nM)^2$$

$$Ka/b_{(Klapp \, vs \, 1/[S])} = 0.03 \, (nM)^{-1}$$

$$Ka_{Klapp \, vs \, [S]} = 4.8 \pm 0.3 \, nM$$

DISCUSSION

Comparative data for IC_{50} values for the inhibition of human erythrocyte AChE by different ChEIs used as experimental therapeutics for Alzheimer's disease have been reviewed by Giacobini [30]. According to his report, the IC_{50} (nM) values are as follows: for BW 284 C51 (18.8), phenserine (22.2), galanthamine (0.35), DDVP (dichlorvos) (800), physostigmine (5.4), tacrine (190), eptastigmine (20), hetopropazine (260), bambuterol (30), and MF 8622 (100). Interestingly, in the current study, we determined that tolserine has an IC_{50} value of 8.13 nM, less than all the described inhibitors with the exception of galanthamine and physostigmine. Galanthamine (lycoremine,

TABLE 3. Kinetic constants estimated by various plots and replots

Plots and replots	K_i (nM)	K_m (mM)	V_{max} (μM/hr/mg)
Primary plot	4.63	0.080	3.70
Secondary replot[1LBP]	4.28	—	5.03
Secondary replot[2LBP]	5.09	—	—
Secondary replot[1DP]	—	0.073	—
Secondary replot[2DP]	—	0.086	3.99
Secondary replot[3DP]	4.34	—	—
Secondary replot[4DP]	5.12	—	—
Mean value	4.69	0.080	4.24
SEM	0.18	0.004	0.40

The details of primary plot and secondary replots are given in the text, while [LBP]signifies Lineweaver–Burk plot and [DP]Dixon plot. [1LBP]represents replot of $1/V_{maxapp}$ versus tolserine concentration and [2LBP]represents replot of slope from Lineweaver–Burk plot versus tolserine concentration (Fig. 4, B and C). [1DP]represents replot of slope from Dixon plot versus 1/[ASCh], [2DP]represents replot of $1/V_{maxapp}$ versus 1/[ASCh] (Fig. 6A), [3DP]represents replot of K_{Iapp} from Dixon plot versus 1/[ASCh] (Fig. 6B), and [4DP]represents replot of K_{Iapp} versus ASCh concentration (Fig. 6C).

TABLE 4. Comparative data for inhibition of erythrocyte AChE by eserine and its derivatives

Eserine and its derivatives	K_i (μM)	Nature of inhibition	P.T.$^{\parallel}$ (min)
Physostigmine*	3.1	Competitive	0.0
Physostigmine*	0.19	Non-competitive	6.8
Physostigmine*	0.10	Non-competitive	18.9
Eseroline†	0.22	Competitive	15.0
Phenserine‡	0.048	Non-competitive (pure)	5.0
Tolserine§	0.0047	Non-competitive (partial)	10.0

*Ref. 46.
†Ref. 47.
‡Ref. 15.
§Current study.
$^{\parallel}$Preincubation time.

Jilkon™) is a natural alkaloid obtained from the common snowdrop *Galanthus nivalis*, having a maximum selectivity for AChE versus BChE (53-fold) compared to phenserine (70-fold selectivity) among the above-described agents. Interestingly, galanthamine has an IC_{50} value of some 2000 nM for rat striatum. In comparison, tolserine has a dramatic selectivity for AChE versus BChE of 200-fold.

If we consider the compound on which tolserine was structurally based, i.e. physostigmine, it similarly has different reported IC_{50} (μM) values against different sources of AChE. For example, against guinea pig whole blood (40) [31], cortex (63), mouse erythrocytes (68), hippocampus (15), frontal cortex (14), temporal cortex (16), human erythrocytes (27) [32], venom of *Walterinnesia aegyptia* (0.03) [33], and the A (95), B (92), and C (28) forms of bovine caudate nucleus tissue [34]. Furthermore, the unfavorable side effect profile of physostigmine, (first potent and natural inhibitor of cholinesterases), which lacks selectivity between the cholinesterase subtypes, is well known along with its short half-life and narrow therapeutic window.

The IC_{100} value for the inhibition of human erythrocyte AChE by tolserine was calculated in the present study to be 25.5 nM. This compares favorably to reported values of the anticholinesterase Alzheimer therapeutic, tacrine, which also has an IC_{100} value of 14,220 nM for the inhibition of camel retina AChE [35]. Hence, human erythrocyte AChE has 558-fold more sensitivity to tolserine than camel retina AChE has to tacrine. In addition, 100% inhibition of AChE from *Ascaridia galli* has been reported by 1.0 and 0.10 mM concentrations of physostigmine [36]. Moreover, comparative data for inhibition of erythrocyte AChE by physostigmine (eserine) and its derivatives and presented in Table 4. These results suggest that the novel compound tolserine is an ideal and potentially leading experimental therapeutic for Alzheimer's disease therapy as compared to other reported drugs and experimental therapeutics under clinical investigation for this disease.

The results of Lineweaver–Burk analysis indicate that tolserine inhibits AChE activity noncompetitively (Fig. 4A). The decrease in V_{max} in the presence of tolserine without any change in the K_m value of AChE suggests that tolserine produces a conformational change in the enzyme. A non-competitive type of inhibition has two subtype forms: partial and pure. These can be distinguished on the basis of replots of $1/V_{maxapp}$ and $slope_{1/ASCh}$ versus tolserine concentration (Fig. 4, B and C). In the present study, we found slightly concave curves (correlation coefficients were 0.98 and 0.97 for $1/V_{maxapp}$ and slope, respectively, after linear regression analysis; not shown), indicating a partial non-competitive subtype form of inhibitor instead of linear plots, as would be found for a pure non-competitive subtype. Interestingly, this contrasts with our prior study of phenserine, whose inhibition of human AChE was determined to be of a pure non-competitive subtype [15].

According to the accepted hydrolysis scheme for acetate substrate by AChE [37], tolserine can interact with AChE at either the AChE–ASCh complex stage or at a regulatory site of the free AChE. This would form a tolserine–AChE complex that would thereby decrease both acylation and deacylation, as the first product of the hydrolysis of ASCh (thiocholine; SCh) was found to be decreased with increasing tolserine concentration as determined by absorption at 412 nm wavelength of 5-thionitrobenzoate (colored anion formed after reaction of SCh with DTNB). In considering the former case of an AChE–ASCh complex, the anionic subsite of AChE is occupied by the choline moiety of the ASCh and hence is not available to bind a second ligand, and tolserine thus binds at the peripheral site of AChE.

However, as described by Kamal [38] for the insecticide, lannate, confusion may occur in cases in which replots of $slope_{1/[ASCh]}$ and $1/V_{maxapp}$ versus inhibitor concentration result in the generation of a slightly concave curve. This indicates a mixed type of inhibition system, composed of a 'semi-pure competitive' and 'semi-partial as well as semi-pure non-competitive' mixture. In the present study of tolserine, we likewise found that slightly concave curve-type plots were generated (Fig. 4, B and C). The slightly concave curve-type shape of a Dixon plot (Fig. 5, A and B) is associated with a recently introduced slightly concave mixed type of inhibition system. The specific type involved can be assessed by comparing the following differences in secondary replots of the Dixon plot (Fig. 6). It will first be noted from Fig. 6A, that the slope values are lower than $1/V_{maxiapp}$ versus $1/[ASCh]$ and then for Fig. 6C, that the values of K_{Iapp} versus [ASCh] are nonsignificantly decreased. These two points occur in reverse order in the case of a slightly concave mixed type of inhibition system [38].

A question thus arises, which is illustrated in Fig. 5C. Theoretically, in the case of a non-competitive type of inhibition, K_{Iapp} should be identical at all concentrations of substrate in the Dixon plot. However, in the current study, as illustrated in Fig. 5C, all lines did not intersect 100% at one point on the abscissa. As a consequence, there was a doubt about the specific type of inhibition. To resolve this, we initially plotted K_{Iapp} values at each substrate concentration against the reciprocal of the substrate concentration (Fig. 6B). This partially resolved the problem, as linear

regression analysis gave a slope with a value of only 0.017 ± 0.015. The K_{Iapp} was thus determined not to be significantly dependent on the reciprocal of the substrate concentration, with a correlation coefficient of 0.49. When, however, the K_{Iapp} values were replotted against the substrate concentration (Fig. 6C), linear regression analysis gave zero slope value (-0.0), with a correlation coefficient of -0.76. In contrast, when this was undertaken with phenserine, we found contrast values of the correlation coefficient in both plots. Hence, tolserine, unlike phenserine [15], is not a pure non-competitive inhibitor of AChE, although the two agents are close analogues differing only in a single methyl group. This analysis is valuable for overcoming confusion regarding the type of non-competitive inhibition of compounds. These results reflect a conformational change in the enzyme by the binding of tolserine with the AChE–ASCh complex, yielding a poorly productive AChE–ASCh–tolserine complex which was not as effective as AChE–ASCh. It is in this latter respect that this partial non-competitive inhibition system is different from a pure non-competitive inhibition, in which the AChE–ASCh–inhibitor complex (i.e. AChE–ASCh–phenserine) proves to be non-productive. In contrast, tolserine proved able to decrease the activity of the enzyme in this manner. Thus, tolserine and ASCh are not mutually exclusive, and both ligands bind independently to the AChE at different sites.

Long-chain analogues of physostigmine (eptastigmine, 8-morpholinooctylphysostigmine and 8-(2,6-dimethylmorpholino)octylphysostigmine) have also been reported to have therapeutic efficacy for AD and to have non-competitive-like kinetics with regards to their inhibition of purified AChE (Type V) electric eel [39], which supports our findings with tolserine in the present study. Prior studies by Atack *et al.* [40] on both aryl and alkyl carbamates of eseroline, similar to compounds in both the present study and in that of Perola *et al.* [39], have shown that their inhibition of human erythrocyte AChE was similar to that achieved against human brain-derived AChE, but often different against AChE derived from electric eel. For example, the IC_{50} values of phenserine against human brain and erythrocyte AChE are 36 ± 3 nM and 24 ± 6 nM, respectively, which contrasts with a value of 350 ± 9 nM for electric eel AChE. We therefore predict that the enzyme kinetics and mode of inhibition determined for phenserine and tolserine against human erythrocyte AChE are similar to those that would occur in brain. Indeed, although AChE appears to be a highly polymorphic protein and can exist in both globular (G) and asymmetric (A) forms, studies reviewed by Soreq and Zakut [6] suggest that the catalytic subunit of AChE is similar in all forms throughout the body. Molecular cloning studies indicate that differences between AChEs from different species, such as humans and eels, and between AChE and BChE may be attributed to primary sequence variations, whereas differences between AChE in different body organs result from posttranslational modifications. These latter modi-

fications provide for regional differences in the arrangement of AChE subunit numbers and in their tethering. In brain, for example, AChE is predominantly in a globular tetrameric (G4) form of which up to 85% is lost in AD [41], whereas it exists in a G2 form in human erythrocytes [42] which is unaffected in AD. The G2 erythrocyte form contains a C-terminal glycolipid anchor, while the G4 form contains a C-terminal T peptide that allows the formation of tetrameric assemblies with a proline-rich attachment domain of collagen [43]. They are encoded by the same gene, but use different exons for the C-terminal peptides. Apart from this, the primary peptide sequence of the catalytic domain is identical, while the difference is due to glycosylation. These studies suggest that assessment of enzyme binding and inhibition kinetics in human erythrocyte AChE, rather than in eel-derived enzyme, is a more appropriate model of human brain AChE, although such kinetics could be altered by the pathological consequences of AD.

It is clear from a comparison of the enzyme kinetics of tolserine and phenserine that an apparently minor difference in the structures of these analogues (a single 2′-methyl substitution within the phenylcarbamoyl moiety) can result in both biochemical and pharmacologic differences. As described, the kinetics of enzyme inhibition together with the specific type of inhibition differ, although both are highly potent and reversible carbamate-type AChE inhibitors. Preliminary molecular modeling studies suggest that substitution in the phenylcarbamate moiety of phenserine results in torsion, causing rotation of the phenyl group in relation to the primary tricyclic ring structure [44]. This modification in its 3-dimensional structure likely results in an altered interaction with AChE and results in the different inhibition kinetics associated with tolserine and phenserine, respectively. The preferred conformation in tolserine provides an AChE selectivity of 200-fold versus 75-fold for phenserine, and maintains the high potency and long *in vivo* duration of stable inhibition. The 2′-methyl substitution additionally increases the hydrophobic properties of tolserine versus phenserine and hence augments its blood–brain barrier permeability [45], thereby providing it with a high brain uptake (brain/plasma concentration ratio of 24:1). Indeed, of the ChEIs that are loosely based on the structure of the first-generation drug, physostigmine, and that have been synthesized to date, tolserine represents one of the most potent and AChE-selective.

Tolserine's favorable features, combining AChE selectivity with a long *in vivo* duration of action, rapid clearance, and high brain versus systemic delivery, clearly make it an interesting third-generation ChEI that is worthy of further preclinical assessment. These characteristics, together with its unusually wide therapeutic window, may prove advantageous in AD treatment to maximize central nervous system cholinergic augmentation, minimize augmentation elsewhere, and test the true therapeutic value of ChEIs in this catastrophic disease.

References

1. Giacobini E, Cholinesterase inhibitors do more than inhibit cholinesterase. In: *Alzheimer's Disease: from Molecular Biology to Therapy* (Eds. Becker R and Giacobini E), pp. 187–204, Birkhauser, Boston, 1997.

2. Kasa P, Rakonczay Z and Gulya K, The cholinergic system in Alzheimer's disease. *Prog Neurobiol* **52:** 511–532, 1997.

3. Deutsch J, The cholinergic synapse and the site of memory. *Science* **313:** 7–11, 1985.

4. Avery EE, Baker LD and Asthana S, Potential role of muscarinic agonists in Alzheimer's disease. *Drugs Aging* **11:** 450–459, 1997.

5. Newhouse PA, Potter A and Levin ED, Nicotinic system involvement in Alzheimer's and Parkinson's diseases. Implications for therapeutics. *Drugs Aging* **11:** 206–208, 1997.

6. Soreq H and Zakut H, Molecular polymorphism and its genomic origin. In: *Human Cholinesterases and Anti-cholinesterases*, pp. 41–45. Academic Press, New York, 1993.

7. Terry RD, Masliah E, Salmon DP, Butters N, DeTeresa R, Hill R, Hansen LA and Katzman R, Physical basis of cognitive alterations in Alzheimer's disease: Synapse loss is the major correlate of cognitive impairment. *Ann Neurol* **30:** 572–580, 1991.

8. Gracon S, Smith F, Hoover T, Knopman D, Schneider L, Davis K and Talwalker S, Long-term tacrine treatment: Effect on nursing home placement and mortality. In: *Alzheimer's Disease: from Molecular Biology to Therapy* (Eds. Becker R and Giacobini E), pp. 205–209. Birkhauser, Boston, 1997.

9. Blackard WG Jr, Sood GK, Crowe DR and Fallon MB, Tacrine. A cause of fatal hepatotoxicity? *J Clin Gastroenterol* **26:** 57–59, 1998.

10. Barner EL and Gray SL, Donepezil use in Alzheimer disease. *Ann Pharmacother* **32:** 70–77, 1998.

11. Becker R, Moriearty P and Unni L, The second generation of cholinesterase inhibitors: Clinical and pharmacological effects. In: *Cholinergic Basis of Alzheimer's Disease* (Eds. Becker R and Giacobini E), pp. 263–296. Birkhauser, Boston, 1991.

12. Yu QS, Holloway HW, Utsuki T, Brossi A and Greig NH, Synthesis of novel phenserine-based-selective inhibitors of butyrylcholinesterase for Alzheimer's Disease. *J Med Chem* **42:** 1855–1861, 1999.

13. Lahiri DK, Farlow MR and Sambamurti K, The secretion of amyloid β-peptides in inhibited in tacrine-treated human neuroblastoma cells. *Mol Brain Res* **62:** 131–140, 1998.

14. Lahiri DK, Farlow MR, Nurnberger JI Jr and Greig NH, Effects of cholinesterase inhibitors on the secretion of beta-amyloid precursor protein in cell cultures. *Ann N Y Acad Sci* **826:** 416–421, 1997.

15. Al-Jafari AA, Kamal MA, Greig NH, Alhomida AS and Perry ER, Kinetics of human erythrocyte acetylcholinesterase inhibition by a novel derivative of physostigmine: Phenserine. *Biochem Biophys Res Commun* **248:** 180–185, 1998.

16. Liston D, Nielsen JA, Villalobos A, Chapin D, Jones SB, Hubbard S, Shalaby I and White WF, CP-118,954: A potent and selective AChE inhibitor. The importance of selective AChE inhibition *in vivo. Proc Soc Neurosci* **20:** 608–611, 1994.

17. Iijima S, Greig NM, Garofolo P, Spangler EL, Heller B, Brossi A and Ingram DK, Phenserine: A physostigmine derivative that is a long-acting inhibitor of cholinesterase and demonstrates a wide dose range for attenuating a scopolamine-induced learning impairment of rats in a 14-unit T-maze. *Psychopharmacology (Berl)* **112:** 415–420, 1993.

18. Patel N, Spangler EL, Greig NH, Yu QS, Ingram DK and Meyer RC, Tolserine, a novel acetylcholinesterase inhibitor, attenuates impaired learning of rats in a 14-unit T-maze induced by blockade of the *N*-methyl-D-aspartate receptor. *Neuroreport* **9:** 171–176, 1998.

19. Selkoe DJ, Alzheimer's disease: A central role of β-amyloid. *J Neuropathol Exp Neurol* **53:** 438–447, 1994.

20. Haroutunian V, Greig NH, Utsuki T, Davis KL and Wallace WC, Pharmacological modulation of Alzheimer's β-amyloid precursor protein levels in the CSF of rats with forebrain cholinergic system lesions. *Mol Brain Res* **46:** 161–168, 1997.

21. Meyer RC, Munoz JR, Patel N, Knox J, Sohn J, Utsuki T, Holloway HW, Greig NH and Ingram DK, Complex maze learning is improved in aged rats treated with novel and long-acting acetylcholinesterase inhibitors. *Neuropharmacoly*, in press.

22. Greig NH, Pei X-F, Soncrant TT, Ingram DK and Brossi A, Phenserine and ring C hetero-analogues: Drug candidates for the treatment of Alzheimer's disease. *Med Res Rev* **15:** 3–31, 1995.

23. Ellman GL, Courtney D, Andres V Jr and Featherstone RM, A new and rapid colorimetric determination of acetylcholinesterase activity. *Biochem Pharmacol* **7:** 88–95, 1961.

24. Al-Jafari AA and Kamal MA, Optimization and kinetic studies of human erythrocyte membrane-bound acetylcholinesterase. *Biochem Mol Biol Int* **38:** 577–586, 1996.

25. Erithacus Software, Hill plot. In: *GraFit User's Guide* (Ed. Leatherbarrow RJ), Version **3.0**, p. 267. Erithacus Software Ltd., Staines, U.K., 1992.

26. Al-Jafari AA, Kamal MA, Duhaiman AS and Alhomida AS, Kinetics of the inhibition of acetylcholinesterase from desert cobra (*Walterinnesia aegyptia*) venom by local anesthetics: Procaine and tetracaine. *J Enz Inhib* **11:** 123–134, 1996.

27. Kamal MA, Nasim FH and Al-Jafari AA, Investigation of the effect of anti-neoplastic drugs, cyclophosphamide, cisplatin and methotrexate on the turnover kinetics of human erythrocyte acetylcholinesterase. *Biochem Mol Biol Int* **39:** 293–302, 1996.

28. Lowry OH, Rosebrough NJ, Farr AL and Randall RJ, Protein measurement with the Folin Phenol reagent. *J Biol Chem* **193:** 265–275, 1951.

29. Leatherbarrow RJ, GraFit. Version **3.0**. Erithacus Software Ltd., Staines, UK, 1992.

30. Giacobini E, From molecular structure to Alzheimer therapy. *Jpn J Pharmacol* **74:** 225–241, 1997.

31. Harris LW, Anderson DR, Pastelak AM, Bowersox SL, Vanderpool BA and Lennox WJ, Acetylcholinesterase inhibition and anti-soman efficacy of homologs of physostigmine. *Drug Chem Toxicol* **15:** 127–143, 1992.

32. Thomsen T, Kaden B, Fischer JP, Bickel U, Barz H, Gusztony G, Cervos-Navarro J and Kewitz H, Inhibition of acetylcholinesterase activity in human brain tissue and erythrocytes by galanthamine, physostigmine and tacrine. *Eur J Clin Chem Clin Biochem* **29:** 487–492, 1991.

33. Duhaiman A, Alhomida AS, Rabbani N, Kamal MA and Al-Jafari AA, Purification and characterization of acetylcholinesterase from desert cobra (*Walterinessia aegyptia*) venom. *Biochimie* **77:** 46–50, 1996.

34. Chan SL, Shirachi DY, Bhargava HN, Gardner E and Trevor AJ, Purification and properties of multiple forms of brain acetylcholinesterase (EC 3.1.1.7). *J Neurochem* **19:** 2747–2758, 1972.

35. Al-Jafari AA, The nature of the inhibition of camel retina acetylcholinesterase (EC 3.1.1.7) activity by tetrahydroaminoacridine. *J Ocul Pharmacol Ther* **12:** 503–513, 1996.

36. Gupta S, Sanyal SN and Duggal CL, Study of the acetylcholinesterase activity of *Ascaridia galli*: Kinetic properties and the effect of anthelmintics. *Acta Vet Hung* **39:** 165–174, 1991.

37. Cohen SG, Chishti SB, Bell DA, Howard SI, Salih E and Cohen JB, General occurrence of binding to acetylcholines-

terase–substrate complex in noncompetitive inhibition and in inhibition by substrate. *Biochim Biophys Acta* **1076:** 112–122, 1991.

38. Kamal MA, Investigation of the effect of lannate on kinetic parameters of acetylcholinesterase: Slightly concave mixed-type of inhibition system. *Biochem Mol Biol Int* **43:** 1183–1193, 1997.

39. Perola E, Cellai L, Lamba D, Filocamo L and Brufani M, Long chain analogs of physostigmine as potential drugs for Alzheimer's disease: New insights into the mechanism of action in the inhibition of acetylcholinesterase. *Biochim Biophys Acta* **1343:** 41–50, 1997.

40. Atack JR, Yu QS, Soncrant TT, Brossi A and Rapoport SI, Comparative inhibitory effects of various physostigmine analogues against acetyl- and butyrylcholinesterase. *J Pharmacol Exp Ther* **249:** 194–202, 1989.

41. Perry EK, Perry RH, Blessed G and Tomlinson BE, Changes in brain cholinesterases in senile dementia of Alzheimer type. *Neuropathol Appl Neurobiol* **4:** 273–277, 1978.

42. Ott P, Lustig A, Brodbeck U and Rosenbusch JP, Acetylcholinesterase from human erythrocyte membrane: Dimers as functional units. *FEBS Lett* **138:** 187–189, 1982.

43. Massoulie J, Anselmet A, Bon S, Krejci E, Legay C, Morel N and Simon S, Acetylcholinesterase: C-terminal domains, molecular forms and functional localization. *J Physiol (Paris)* **92:** 183–190, 1998.

44. Yu QS, Holloway HW, Brossi A and Greig NH, Substituted phenserine: Syntheses and anti-cholinesterase structure/activities relationships. *J Med Chem*, in press.

45. Greig NH, Drug entry to the brain and its pharmacologic manipulation. In: *Handbook of Experimental Pharmacology* (Ed. Bradbury MW), Vol 103, pp. 487–523. Springer-Verlag, Heidelberg, Germany, 1992.

46. Stein HH and Lewis GJ, Noncompetitive inhibition of acetylcholinesterase by eserine. *Biochem Pharmacol* **18:** 1679–1684, 1969.

47. Galli A, Renzi G, Grazzini E, Bartolini R, Aiello-Malmberg P and Bartolini A, Reversible inhibition of acetylcholinesterase by eseroline, an opioid agonist structurally related to physostigmine (eserine) and morphine. *Biochem Pharmacol* **31:** 1233–1238, 1982.

48. Segel IH, Rapid equilibrium partial and mixed-type inhibition. In: *Enzyme Kinetics: Behavior and Analysis of Rapid Equilibrium and Steady State Enzyme Systems*, pp. 166–169. J Wiley, New York, 1975.